1 Seawater- freshwater interface web-based tool based on analytical solutions compared with SEAWAT code

Mohamed Selmy[1], Hewida Omara[1], Bakenaz A. Zeidan[1], Asaad M. Armanuos[1], and Sobhy R. Emara*[1]

[1]Irrigation and Hydraulics Engineering Department, Faculty of Engineering, Tanta University, Tanta, Egypt, Email: mohamed.selmy@f-eng.tanta.edu.eg, hewida.omara@f-eng.tanta.edu.eg, b.zeidan@f-eng.tanta.edu.eg, asaad.matter@f-eng.tanta.edu.eg, sobhy_emara39@f-eng.tanta.edu.eg

*Correspondence: sobhy_emara39@f-eng.tanta.edu.eg

ABSTRACT

Seawater intrusion (SWI) is a common environmental problem threatening freshwater in coastal aquifers worldwide. The main objective of this study is to introduce the changes in the seawater-freshwater interface using different available analytical solutions through a web-based interface tool. Two case studies include a hypothetical unconfined coastal aquifer and real case study of Gaza coastal aquifer was applied to check the variations of the saltwater-freshwater interface through the built seawater-freshwater interface tool using JavaScript language. To simulate variable density flow in the Gaza coastal aquifer, the SEAWAT code was employed. The resulting seawater intrusion lengths simulated by SEAWAT were compared with those obtained from the web-based analytical solutions under both constant flux and constant head boundary conditions. The comparison revealed a strong agreement between the SEAWAT model results and the analytical solutions. This study provides valuable insights into seawater intrusion in coastal aquifers, with a particular focus on the impact of sea level rise (SLR) on the shifting location of the seawater intrusion toe. The findings are presented through an accessible web-based interface, facilitating wider dissemination and practical application of the research outcomes.

1 KEYWORDS

Saltwater Intrusion, Numerical Simulation, Coastal Aquifers, Sea Level Rise, and SEAWAT.

2 INTRODUCTION

Seawater intrusion (SWI), the contamination of coastal groundwater with saline seawater, poses a significant threat to coastal habitats globally, especially in areas where groundwater is the primary freshwater source. Normally, groundwater discharges towards the sea, preventing salinity intrusion into aquifers. However,

excessive groundwater extraction can lower groundwater levels, diminishing freshwater discharge and exacerbating SWI effects (Emara et al., 2024a; Werner et al., 2013). Thus, effectively managing and comprehending coastal aquifers are vital aspects of ensuring global water security.

Climate change significantly influences saltwater intrusion in multiple ways. Directly, it causes sea level rise (SLR). Indirectly, it leads to reduced rainfall in some regions, resulting in decreased natural recharge and drought. These impacts cause the saltwater wedge to move further inland, a problem worsened by excessive groundwater withdrawal (Ataie-Ashtiani et al., 2013; Abdoulhalik and Ahmed, 2017; Emara et al., 2023a).

Saltwater intrusion due to sea-level rise is currently a significant threat to global freshwater resources (Dang et al., 2020). In modeling seawater intrusion, both analytical solutions (Ataie-Ashtiani et al., 2013; Lu et al., 2016) and numerical modeling (Sherif et al., 2014; Abd-Elaty and Zelenakova, 2022; Emara et al., 2024b) are effective methods.

In a sloping coastal unconfined aquifer with a constant recharge rate, Koussis et al. (2012) developed steady-state analytical solutions to determine the position of the interface toe under the assumption of a sharp-interface SWI. Lu et al. (2015) formulated analytical solutions for SWI in both unconfined and confined coastal aquifers, incorporating an inland general-head boundary condition. They used these solutions to predict the movement of the interface toe in response to a 1-meter SLR. Lu et al. (2016) also derived steady-state analytical solutions for SWI in sloping unconfined and confined aquifers, again assuming a sharp-interface SWI.

In an anisotropic aquifer of specified depth, Anderson (2021) provided an analytical solution for the discharge of the unconfined coastal interface. Luo et al. (2022) derived analytical solutions for steady-state SWI in unconfined coastal aquifers based on the sharp-interface assumption, solving the discharge equation analytically while accounting for unsaturated flow.

Emara et al.(2023a) combined numerical and experimental methods to investigate SWI in two homogeneous aquifers under conditions of sea level rise and varying freshwater inputs. The research compares transient groundwater heads and salt concentrations from numerical models with experimental data for both receding and advancing fronts. Ten steady-state SWI wedge and toe length experimental tests were evaluated against seven

analytical solutions. The study highlights the significant impact of inland water head and sea level rise on SWI dynamics.

Ataie-Ashtiani et al. (2013) employed a direct analytical method to measure the impact of land-surface inundation on SLR-SWI dynamics in simplified settings. The results indicate that land-surface inundation significantly expands SWI boundaries, potentially resulting in inland penetration several times greater than shoreline pressure alterations in open coastal aquifers with realistic conditions.

Goswami and Clement (2007) created a benchmark model for seawater intrusion through lab-scale experiments, exploring the saltwater wedge's movement in both steady-state and transient conditions. Chang et al. (2011) showed that changes in freshwater discharges and rising sea levels can affect both confined and unconfined aquifers. Kuan et al.(2012) explained how regional variations in freshwater inflow and tide patterns impact SWI in coastal aquifers.

Armanuos et al. (2019) explored ways to mitigate seawater intrusion (SWI) by using cutoff walls, recharge wells, or both together, utilizing the SEAWAT code. They discovered that combining freshwater injection with physical barriers was the most effective method. This approach significantly pushed back seawater, achieving higher repulsion ratio values than using either a cutoff wall or freshwater injection alone.

To prevent saltwater intrusion and preserve groundwater quality in coastal areas, researchers have suggested several engineering solutions. These include optimizing pumping well layouts (Fan et al., 2020; Ranjbar et al., 2020), using positive hydraulic barriers like artificial recharge through infiltration or injection (Motallebian et al., 2019; Armanuos et al., 2020a), employing negative hydraulic barriers such as inland saltwater pumping (Javadi et al., 2015; Mehdizadeh et al., 2019), and constructing underground physical barriers (Kaleris and Ziogas, 2013; Armanuos et al., 2020b; Emara et al., 2023b).

The main objective of this study is to introduce the changes in the seawater-freshwater interface using different available analytical solutions through a web-based interface tool. Two case studies include a hypothetical unconfined coastal aquifer (Sun et al., 2021) and real case study of Gaza coastal aquifer was applied to check the variations of the saltwater-freshwater interface through the built seawater-freshwater interface tool using JavaScript language. SEAWAT code was applied to simulate the variable density flow in Gasa coastal aquifer.

3 METHODOLOGY AND MODELING

In this research, SEAWAT was implemented to develop numerical models of salt transport in groundwater flow within coastal aquifers. The simulated saltwater intrusion wedge produced by SEAWAT was validated against analytical solutions. Specifically, the simulated intrusion lengths were compared with the analytical solutions of Ataie-Ashtiani et al. (2013) for both constant flux and constant head boundary conditions. The research includes two case studies: a hypothetical unconfined coastal aquifer (Sun et al., 2021) and the Gaza coastal aquifer in Palestine. The steady-state seawater wedges resulting from these simulations were compared with analytical solutions developed by Ghyben (1888), Glover (1959), Rumer Jr and Harleman (1963), and Verruijt (1968). The study particularly focused on the Gaza coastal aquifer, where the simulated intrusion lengths of the saltwater wedge toe, as obtained using the SEAWAT code, were compared with the values calculated by Ataie-Ashtiani et al. (2013). This comparison was facilitated through a web-based interface tool, which also allowed for the examination of various sea level rise scenarios.

3.1 Numerical Model (SEAWAT)

To simulate groundwater variable-density flow, SEAWAT has been used extensively (Guo and Langevin, 2002). SEAWAT was used in the current study to construct a numerical model of salt transport to assess the effect of SLR on groundwater in coastal aquifers.

3.1.1 Governing Equations

Equations (1) and (2), respectively, depict the flow and transport equations used in the SEAWAT.

$$\frac{\partial}{\partial\alpha}\left(\rho k_{f\alpha}\left[\frac{\partial h_f}{\partial\alpha}+\frac{\rho-\rho_f}{\rho_f}\frac{\partial Z}{\partial\alpha}\right]\right)+\frac{\partial}{\partial\beta}\left(\rho k_{f\beta}\left[\frac{\partial h_f}{\partial\beta}+\frac{\rho-\rho_f}{\rho_f}\frac{\partial Z}{\partial\beta}\right]\right)+\frac{\partial}{\partial\gamma}\left(\rho k_{f\gamma}\left[\frac{\partial h_f}{\partial\gamma}+\frac{\rho-\rho_f}{\rho_f}\frac{\partial Z}{\partial\gamma}\right]\right) = \rho S_f\frac{\partial h_f}{\partial t}+\theta\frac{\partial\rho}{\partial C}\frac{\partial C}{\partial t}-\rho_s q_s \quad (1)$$

where α, β, and γ are the direction of groundwater flow; t is the time; $k_{f\alpha}$, $k_{f\beta}$ and $k_{f\gamma}$ are the hydraulic conductivity in the three directions, respectively; θ is the effective porosity;S_f is the specific storage; ρ_f is the freshwater density; ρ is the groundwater density at a point in the aquifer; $q_S$and ρ_S represent the volume and density of the dissolved material, respectively.

$$\frac{\partial(\theta C^k)}{\partial t} = \nabla\left(\theta D_{ij} \nabla C^k\right) - \nabla\left(\theta V_i C^k\right) + q_S C_k^S + \sum R_n \quad (2)$$

where C^k is the solute substance concentration; $\sum R_n$ is the chemical substance reaction term in the aquifer; D represents the coefficient tensor of hydrodynamic dispersion; V_i is the fluid average linear velocity; C_k^S is the value of the source or sink concentration of species k.

3.2 Steady State Analytical Equations

The resulted steady-state seawater wedges were compared with the analytical solutions developed by Ghyben (1888), Glover (1959), Rumer Jr and Harleman (1963), and Verruijt (1968).

Badon Ghyben (1888) and Herzberg (1901) independently derived an analytical equation for determining the sharp interface position between saltwater and freshwater. Their equation correlates the elevation of the saltwater-freshwater interface with the water table elevation in an unconfined aquifer. Later, Glover (1959) formulated an expression to describe the SWI sharp interface in a coastal aquifer, taking into account the seaward flow of freshwater, which could be used to calculate the interface position. Building on Glover's work, Rumer Jr and Harleman (1963) analyzed the parabolic shape of the interface. Verruijt (1968) further demonstrated that the seawater-freshwater interface follows a parabolic profile.

Table 1 presents the analytical equations for seawater- freshwater interface for the following solutions: Ghyben (1888) & Herzberg (1901), Rumer Jr and Harleman (1963), and Verruijt (1968). Table 2 presents the analytical equations of Ataie-Ashtiani et al. (2013) for the impact of Sea Level Rise (SLR) on toe of seawater (SW) - freshwater (FW) interface analytical equations for the Constant Flux Boundary problems and the Constant Head Boundary conditions respectively.

Table 1 Seawater (SW)-Freshwater (FW) Interface Web- Based Model Analytical Equations

Seawater (SW)-Freshwater Interface Web- Based Model Analytical Equations	
Badon Ghyben (1888) & Herzberg (1901)	$z = \frac{\rho_f}{\rho_s - \rho_f} h_f$
Glover (1959)	$z^2 = \frac{2\,\rho_f\,q\,x}{\Delta\rho\,K} + \left(\frac{\rho_f\,q}{\Delta\rho\,K}\right)^2$

Rumer Jr and Harleman (1963)	$z^2 = \frac{2\,\rho_f\,q\,x}{\Delta\rho\,K} + 0.55\left(\frac{\rho_f\,q}{\Delta\rho\,K}\right)^2$
Verruijt (1968)	$Z = -\left(\left(\frac{q}{\beta\,K}\right)^2 \cdot \left(\frac{1-\beta}{1+\beta}\right) + 2\left(\frac{q}{\beta\,K}\right) \cdot \left(\frac{x}{1+\beta}\right)\right)^{1/2}$
Where: ρ_s (M L^{-3}) is the density of saltwater, ρ_f (M L^{-3}) is the density of freshwater, z (L) is the depth of a point on the interface below sea level, and h_f (L) is the elevation of the water table above sea level at that point, q (L^2 T^{-1}) is the freshwater discharge rate, K (LT^{-1}) is the aquifer hydraulic conductivity, $\Delta\rho = \rho_s - \rho_f$, x (L) is the distance from the shoreline and $\beta = (\rho_s - \rho_f)/\rho_f$.	

Table 2 Impact of Sea Level Rise (SLR) on Toe of Seawater (SW) - Freshwater (FW) Interface Analytical Equations, Ataie-Ashtiani et al. (2013)

Constant Flux Boundary	Steady-state SWI toe	$X_T = \left(\frac{q}{W} + L\right) - \sqrt{\left(\frac{q}{W} + L\right)^2 - \frac{K\delta(1+\delta){z_o}^2}{W}}$
	Impact of SLR on the toe of SW-FW interface	$X'_T = \left(\frac{q}{W} + L - \frac{\Delta z}{s}\right) - \sqrt{\left(\frac{q}{W} + L - \frac{\Delta z}{s}\right)^2 - \frac{K\delta(1+\delta)(z_o+\Delta z)^2}{W}} + \frac{\Delta z}{s}$
Constant Head Boundary	Steady state SWI toe	$q = \frac{K((h_b+z_o)^2 - (1+\delta){z_o}^2)}{2L} - \frac{WL}{2}$
		$X_T = \left(\frac{q}{W} + L\right) - \sqrt{\left(\frac{q}{W} + L\right)^2 - \frac{K\delta(1+\delta){z_o}^2}{W}}$
	Impact of SLR on toe of SW-FW interface	$q = \frac{K((h_b+z_o)^2 - (1+\delta)(z+\Delta z)^2)}{2(L - \frac{\Delta z}{s})} - \frac{W(L - \frac{\Delta z}{s})}{2}$
		$X'_T = \left(\frac{q}{W} + L - \frac{\Delta z}{s}\right) - \sqrt{\left(\frac{q}{W} + L - \frac{\Delta z}{s}\right)^2 - \frac{K\delta(1+\delta)(z_o+\Delta z)^2}{W}} + \frac{\Delta z}{s}$

Where: X_T (L) is the position of the toe measured from the sea boundary, z (L) is the sea level rise, X'_T (L) is the new position of the toe measured from the sea boundary after Sea Level Rise (SLR), K (L T^{-1}) is hydraulic conductivity of the aquifer, L (L) is the length of the aquifer length, q (L^2 T^{-1}) is the freshwater flow through the coastal boundary per unit width of coastline, z_o (L) is the depth of aquifer bottom measured from mean sea level, W (L T^{-1}) is the rate of uniform recharge, and δ (−) is the dimensionless density term equal to $(\rho_s-\rho_f)/\rho_f$, where ρ_f (M L^{-3}) is the density of the freshwater and ρ_s (M L^{-3}) is the density of the seawater, s (−) is the slope of the aquifer's seaward boundary. The common value of 0.025 is adopted for δ.

3.3 Case studies

Two case studies for the application of the seawater-freshwater interface web-based tool. Firstly, the seawater-freshwater interface of a hypothetical unconfined coastal aquifer (Table 3) produced from the analytical equations by Ghyben (1888), Glover (1959), Rumer Jr and Harleman (1963), and Verruijt (1968) through the SW-FW web-based tool were compared with the numerical solutions. Secondly, the toe location of the seawater-freshwater interface for the Gaza coastal aquifer resulted from the SEAWAT code was compared with the analytical solution using Ataie-Ashtiani et al. (2013) through the SW-FW interface web-based tool.

Table 3 Numerical solution parameters of the hypothetical unconfined coastal aquifer, Sun et al. (2021)

Parameter	Description	Value	Units
L	Aquifer length	500	m
H	Aquifer depth	50	m
n	Porosity	0.30	
K	Hydraulic conductivity	30	m/day
α_l	Longitudinal dispersivity	1.0	m
α_t	Transverse dispersivity	0.1	m
ρ_f	Freshwater density	1000	Kg/m^3
ρ_s	Saltwater density	1025	Kg/m^3
Boundary condition			
h_s	Seawater hydraulic head	50	m
q_f	Freshwater inflow	0.2	m/day
C_s	Saltwater concentration	35000	mg/L
C_f	Freshwater concentration	1000	mg/L

The Gaza Strip (GS) is a slender coastal region situated along the Mediterranean Sea plain, between Egypt and Palestine. The territory is delimited by longitudes 34° 13′ and 34° 33′ east and latitudes 31° 13′ and 31° 36′ north, and covers an area of 365 square kilometers, boasting a coastline of 45 kilometers. Its width ranges from 6 to 12 kilometers from north to south, with an average width of 9 kilometers (Heen and Muhsen, 2016), as depicted in Figure 1. The GS stands as one of the world's most densely populated areas (Abd-Elaty and Zelenakova, 2022). The heightened demand for groundwater resources will lead to increased abstraction from the aquifer, ultimately resulting in seawater intrusion.

a) Location map of the Gaza Strip

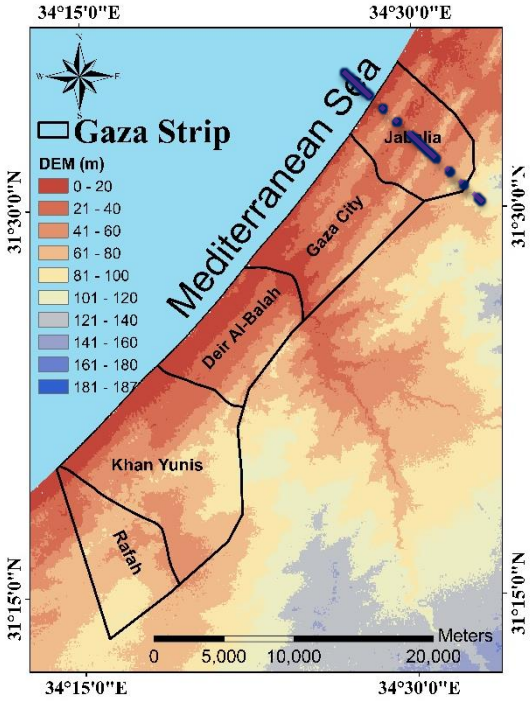

b) Vertical hydrogeological cross-section (Abd-Elaty and Zelenakova, 2022)

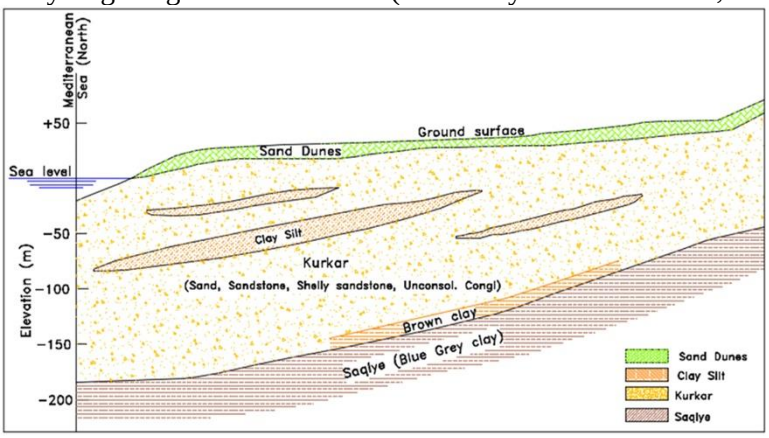

Figure 1 Gaza shallow coastal aquifer

Abualtayef *et al.* (2017) assessed the hydraulic properties of the quaternary aquifer through on-site investigations and pumping tests, determining its hydraulic characteristics. The transmissivity values were estimated to range from 700 m²/day to 5000 m²/day, while the hydraulic conductivity varied from 20 m/day to 80 m/day. For the unconfined aquifer, the specific yield was determined to be within the range of 0.15 to 0.30. In contrast, the confined units exhibited a specific storage value of 10^{-4} m^{-1}. Qahman (2004) estimated the effective porosity to be 0.35, and the longitudinal dispersivity (α_L) and transverse dispersivity (α_T) to be 50m and 0.10m, respectively. Table 4 presents the hydraulic parameters and boundary conditions for the Gaza coastal aquifer.

Table 4 Hydraulic parameters and boundary conditions for Gaza aquifer

Hydraulic parameters	Confined aquifer	Unconfined aquifer	Unit
Horizontal hydraulic conductivity (K_h)	0.2	34	m/day
Vertical hydraulic conductivity (K_v)	0.02	3.4	m/day
Effective porosity (n_e)	0.3	0.25	-
Total Porosity (n_t)	0.45	0.35	-
Freshwater density	1000	1000	Kg/m^3
Saltwater density	1025	1025	Kg/m^3
Specific storage	0.00001	0.0001	-
Longitudinal dispersivity	50	12	-
Transverse dispersivity	5	1.2	-
Molecular diffusion coefficient (D)	0.0001	0.0001	m^2/day
Boundary condition	Value		Unit
Lateral freshwater flux	10		$m^3/day/m$
Well abstraction rates	20.75		$m^3/day/m$
Vertical recharge and return flow	416.5		mm/year
Saltwater head hs	Zero		m
Sea-side concentration	35000		mg/L

Land-side concentration	1000	mg/L

4 Results and Discussion

4.1 Results of seawater-freshwater interface web-based code for hypothetical coastal aquifer

Figure 2 shows the input parameters for the seawater-freshwater interface for the following solutions: Gyhben Herzberg, Glover, Rumer-Herleman, and Virruijt, respectively. The input parameters include the aquifer length, the aquifer depth measured from the sea level to the bottom of the aquifer, the density of freshwater, the density of saltwater, the freshwater flux boundary, and the hydraulic conductivity. For the hypothetical unconfined coastal aquifer, the following are the assigned input parameters: L=500m, H=50m, freshwater density=1.0 gm/cm^3, saltwater density=1.025 gm/cm^3, K=0.000347 cm/sec, and Q=2.31x10^{-6} m^3/sec. The step value is the distance in the x-axis where the depth of the interface is calculated by the different solutions. The assigned step value is 25m. The seawater-freshwater interface is presented in Figure 3 for the following analytical solutions: Gyhben Herzberg, Glover, Rumer-Herleman, and Virruijt respectively. The intrusion length of the saltwater is measured from the saltwater boundary. The calculated length of seawater wedge toe equals 375.021 m, 350.335 m, 350.09 m, and 382.75m for Gyhben Herzberg, Glover, Rumer-Herleman, and Virruijt respectively. The simulated value of toe length by Sun et al. 2021 for the same hypothetical unconfined coastal aquifer equals 340m. Figure 4 presents a comparison between the simulated seawater-freshwater interface for the hypothetical unconfined coastal aquifer by (Sun et al. 2011) and the analytical solutions for Gyhben Herzberg, Glover, Rumer-Herleman and Virruijt through the web-based interface model. Comparison between the simulated and analytical results of the seawater-freshwater interface showed a good agreement. In addition, Glover and Rumer-Herleman present the most accurate solution with respect to the seawater intrusion wedge toe and the seawater intrusion wedge toe penetration length.

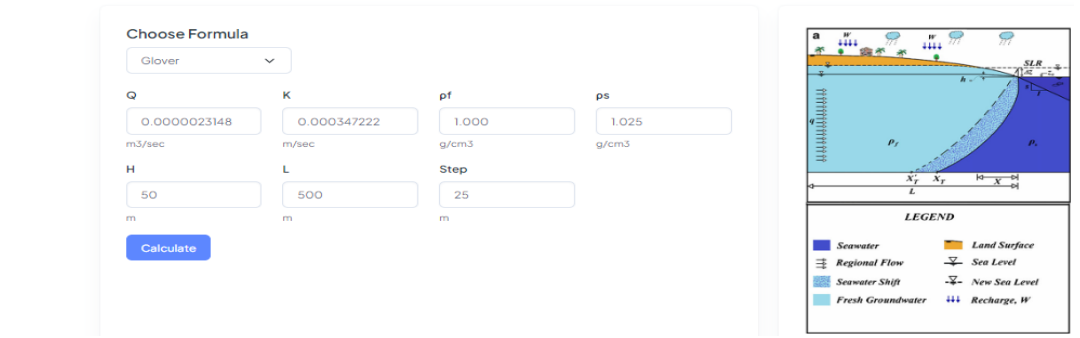

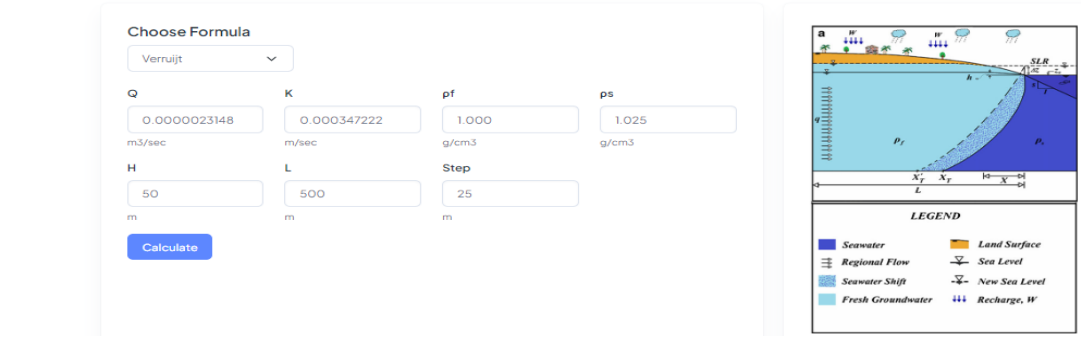

Figure 2 Input Parameters for the seawater-freshwater interface for the following solutions (a) Gyhben Herzberg, (b) Glover, (c) Rumer-Herleman and (d) Virruijt

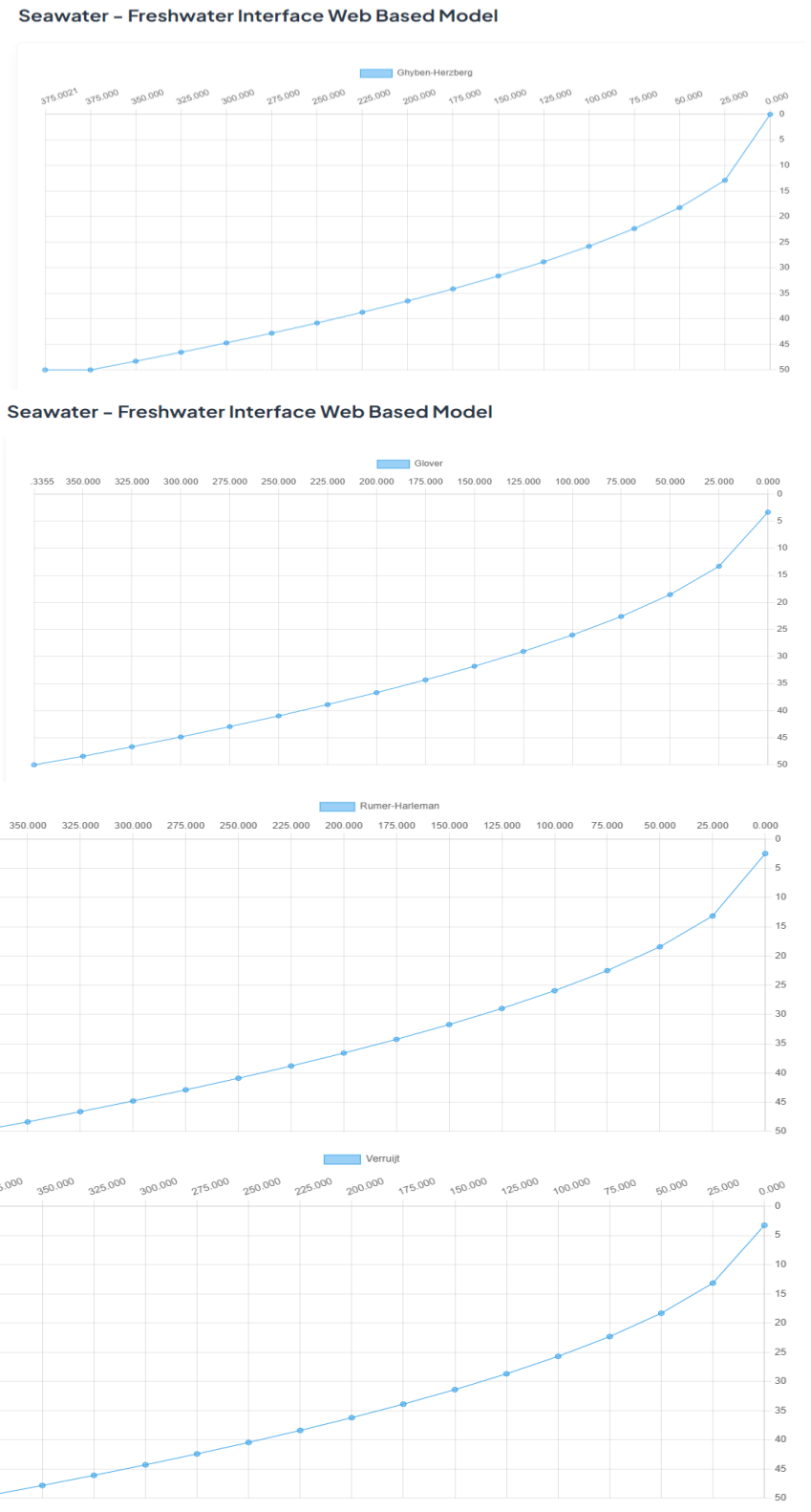

Figure 3 Seawater-freshwater interface based on the following solutions: (a) Gyhben Herzberg, (b) Glover, (c) Rumer-Herleman and (d) Virruijt

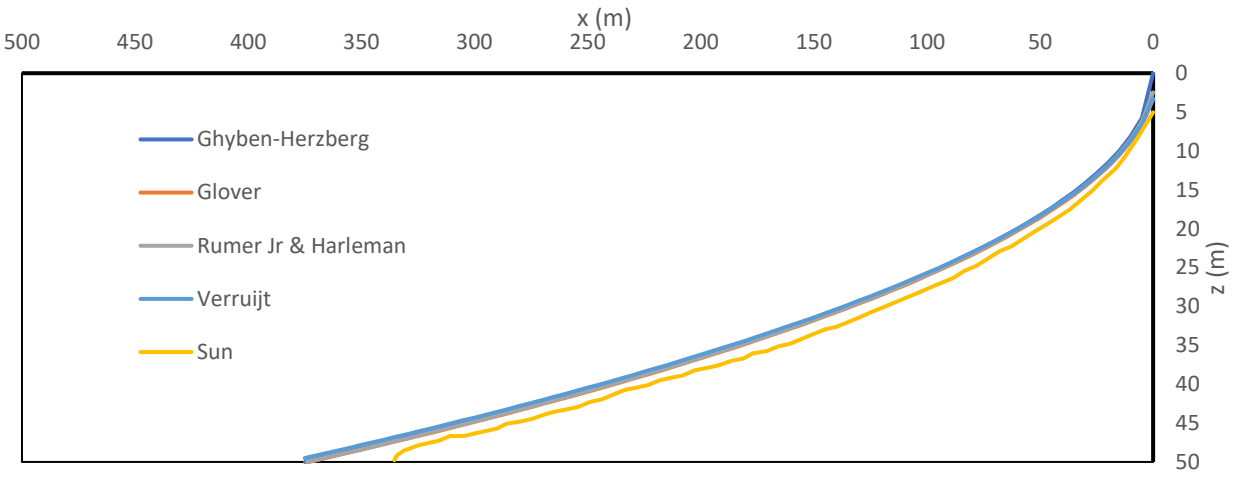

Figure 4 Comparison between the simulated SW- FW interface for the hypothetical unconfined coastal aquifer by (Sun et al. 2011) and the analytical solutions for Gyhben Herzberg, Glover, Rumer-Herleman and Virruijt through the web-based interface model

4.2 Results of the impact of sea level rise on the seawater intrusion in Gaza coastal aquifer, Palestine

The intrusion in GCA was measured to be 3165, 4760, and 5450 m for equi-concentration lines of 32400 ppm (Salt Concentration = 90 %), 18000 ppm (Salt Concentration = 50 %), and 3600 ppm (Salt Concentration = 10 %), respectively (refer to Figure 5)

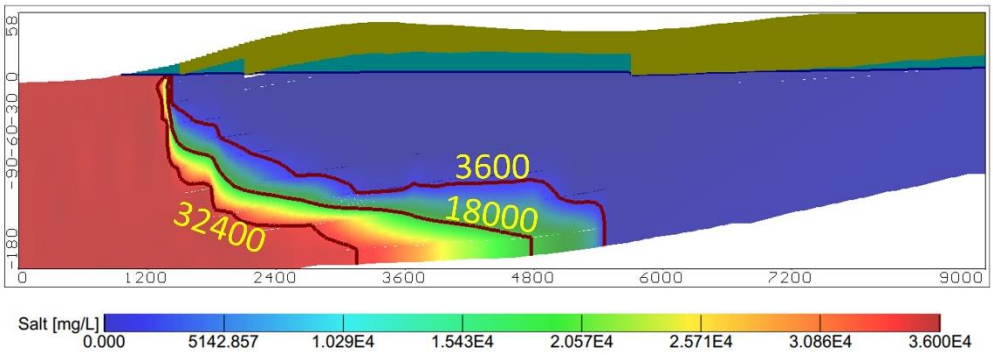

Figure 5 SWI in Gaza aquifer for the base case

Figure 6 displays the input parameters for the calculation of seawater intrusion wedge toe for the Gaza coastal aquifer using Ataie-Ashtiani et al. (2013) through the web-based interface tool for the constant flux boundary problem. For the constant flux boundary sweater intrusion problems, the flux boundary condition is known. The input parameters include the aquifer length, the aquifer depth measured from the sea level to the bottom of the

aquifer bed, the density of freshwater, the density of saltwater, the freshwater flux boundary, the hydraulic conductivity of the aquifer medium, and the rate of recharge. For the Gaza coastal aquifer, the following are the assigned input parameters: L=1000m, Z_o=100m, freshwater density=1.0 gm/cm^3, saltwater density=1.025 gm/cm^3, K=0.15 m/day, and Q=1.7 m^2/day/m. Figure 7 shows the input parameters for the calculation of seawater intrusion wedge toe for the Gaza coastal aquifer using Ataie-Ashtiani et al. (2013) through the web-based interface tool for constant head boundary problems. For the constant head boundary sweater intrusion problems, the flux boundary condition is unknown and the freshwater head above the mean sea level is known. Firstly, through the built web interface the flux boundary condition is calculated based on the input parameters and then the toe location is calculated. The input parameters include the aquifer length, the aquifer depth measured from the sea level to the bottom of the aquifer bed, the density of freshwater, the density of saltwater, and the freshwater head above mean sea level, the hydraulic conductivity of the aquifer medium, and the rate of recharge. For the Gaza coastal aquifer, the following are the assigned input parameters: L=1000m, Z_o=100m, freshwater density=1.0 gm/cm^3, saltwater density=1.025 gm/cm^3, K=0.15 m/day, and h_f=16m. At Z_o=100m, the calculated intrusion wedge toe measured from the sea boundary equals m, m for constant flux boundary and constant head boundary respectively.

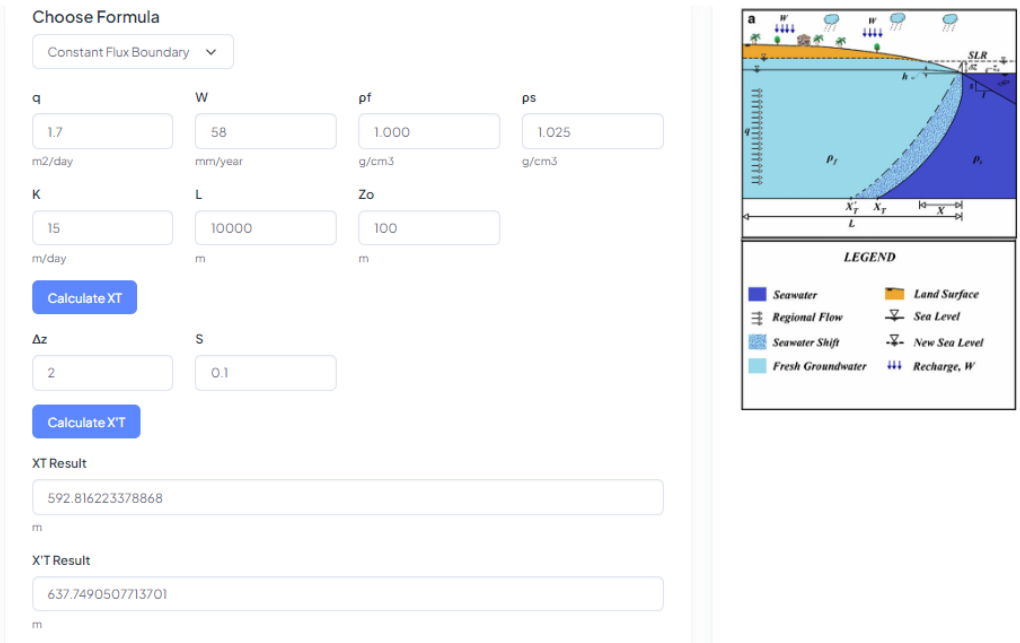

Figure 6 Input Parameters for calculation of seawater intrusion wedge toe for Gaza coastal aquifer using Ataie-Ashtiani et al. (2013)through the web-based interface tool for constant flux boundary problem

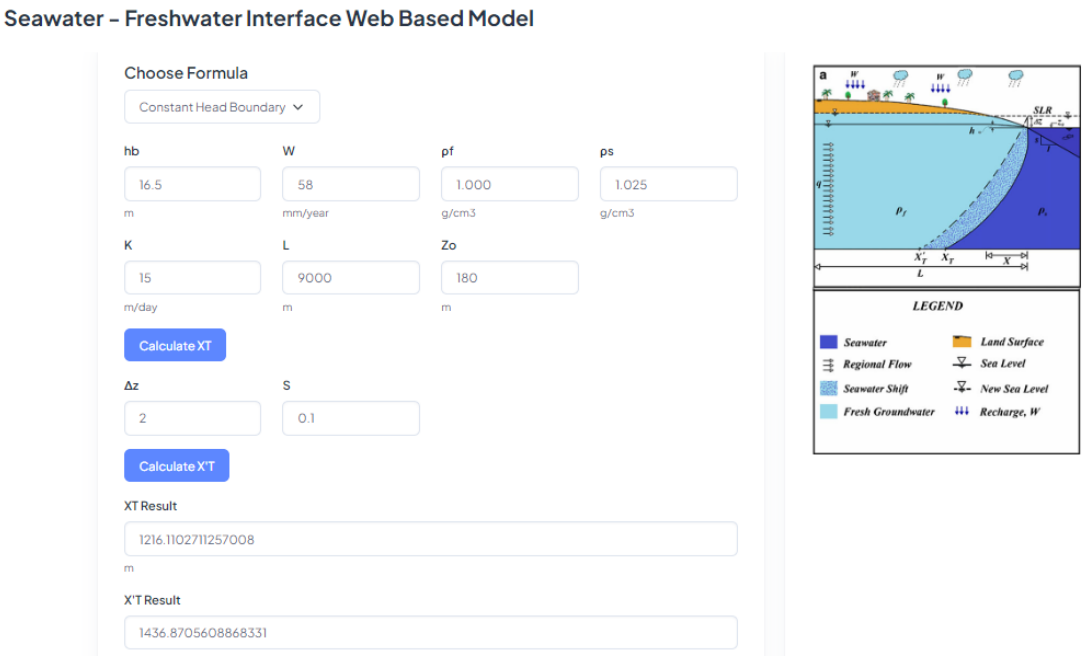

Figure 7 Input Parameters for calculation of seawater intrusion wedge toe for Gaza coastal aquifer using Ataie-Ashtiani et al. (2013) through the web-based interface tool for constant head boundary problem

Also, the web-based built interface calculated the new location of seawater intrusion wedge toe with respect to sea level rise scenarios ΔZ. Table 5 shows the input parameters for the Gaza coastal aquifer and the seawater-freshwater web-based toe position for (Z_o=100m) compared with Ataie-Ashtiani et al. (2013) for different scenarios of sea level rise. The new needed input data to calculate the impact of sea level rise on the location of seawater intrusion wedge toe are the mean seal level ΔZ and the slope of the sea boundary. Table 5 shows the comparison between the intrusion length for the Gaza coastal aquifer by Ataie-Ashtiani et al. (2013) and the resulting calculated value through the web-based interface tool. The results showed a good agreement for sea level rise equals 2.0m and different values of sea slope boundary. The good agreement between the two results is obvious for the two presented cases of constant flux boundary and constant head boundary problems.

Table 5 Parameters for the Gaza Coastal Aquifer and SW-FW web-based toe position for (Z_o=100m) compared with Ataie-Ashtiani et al. (2013)

No.	K (m/day)	W (mm/year)	Z_o (m)	L (m)	ΔZ	S	Flux BC			Head BC		
							Q (m^2/day)	X_T Ataie-Ashtiani et	X_T Current study	h_b (m)	X_T Ataie-Ashtiani et al. (2013)	X_T Current study

								al. (2013)				
1	15	58	100	10000	0	-	1. 7	593	592.8	16.5	593	593.34
					2	0.1		638	637.75		704	703.81
					2	0.01		823	823.34		878	877.71
2	15	31	100	10000	0	-	3.4	454	454.34	23.9	454	454.20
					2	0.1		493	492.97		529	529.49
					2	0.01		675	674.70		702	702.15
3	15	31	100	10000	0	-	1.8	734	734.06	15	734	732.19
					2	0.1		785	784.59		885	884.99
					2	0.01		969	969.14		1055	1054.59

Table 6 presents the input parameters for the Gaza coastal aquifer and seawater- freshwater web-based toe position compared with SEAWAT for (Z_o=180m) (90 % concentration=32400 mg/L) for various scenarios of SLR. Different scenarios of sea level rise are 0.5, 1.0, 1.5, and 2.0 m, checked through the web-based interface and compared with the simulated intrusion length using SEAWAT code. The comparison between the calculated and simulated penetration length of the wedge toe showed a good agreement for different scenarios of sea level rise. The calculated values of seawater intrusion toe length through the web-based tool equals 2101, 2119, 2137, 2155, and 2173 m for the assigned SLR scenarios equals 0.5, 1.0, 1.5, and 2.0 respectively compared with 2101 for steady-state conditions. On the other hand, simulated values of seawater intrusion toe length using SEAWAT code equals 2216, 2229, 2243, and 2252 m for the assigned SLR scenarios equals 0.5, 1.0, 1.5, and 2.0 respectively compared with 2208 m for steady state condition. Figure 8 shows the seawater intrusion distribution in the Gaza coastal aquifer for the steady state condition, SLR=0.5m, SLR=1.0m, SLR=1.5m, and SLR=2.0m respectively. Increasing the sea level causes the seawater to intrude more inland into the Gaza coastal aquifer. The saltwater intrudes more with distances 8, 21, 35, and 44 m respectively in case the sea level rises by 0.5, 1.0, 1.5, and 2.0 m respectively in respect to the SEAWAT code results. In addition, the seawater advances more with distances 18, 36, 54, and 72 m respectively in case the sea level rises by 0.5, 1.0, 1.5, and 2.0 m respectively with respect to the calculated value by Ataie-Ashtiani et al. (2013) through the web-based interface tool.

Table 6 Parameters for the Gaza Coastal Aquifer and SW-FW web-based toe position compared with SEAWAT for (Z_o=180m) (90 % concentration=32400 mg/L) for various scenarios of SLR

No.	K (m/day)	W (mm/year)	Z_o (m)	L (m)	ΔZ	S	Flux BC		
							Q (m^2/day)	SEAWAT	X_T Current Study (m)
1	15	58	180	9000	0	-	1.7	2208	2101
					0.5	0.1		2216	2119
					1.0	0.1		2229	2137
					1.5	0.1		2243	2155
					2.0	0.1		2252	2173

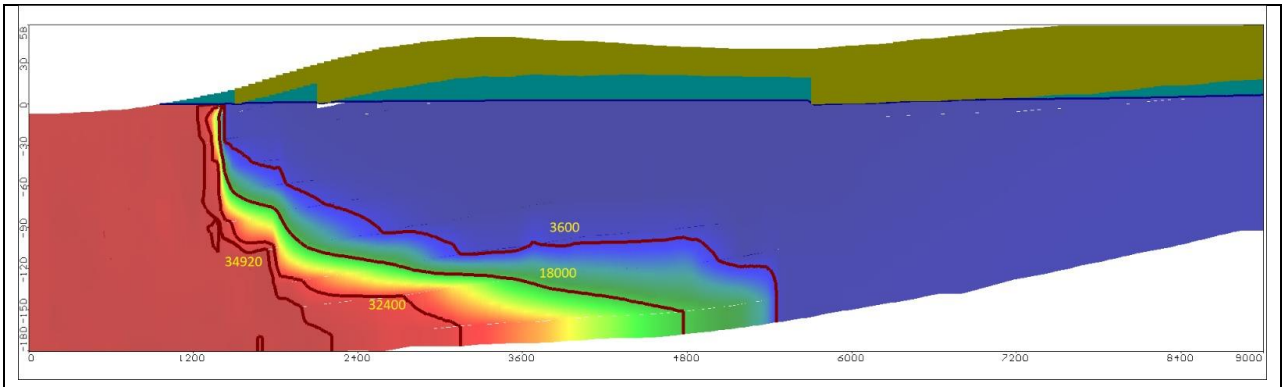

(a) Steady state SWI (X_t= 2208 m of 97% =34920 mg/L)

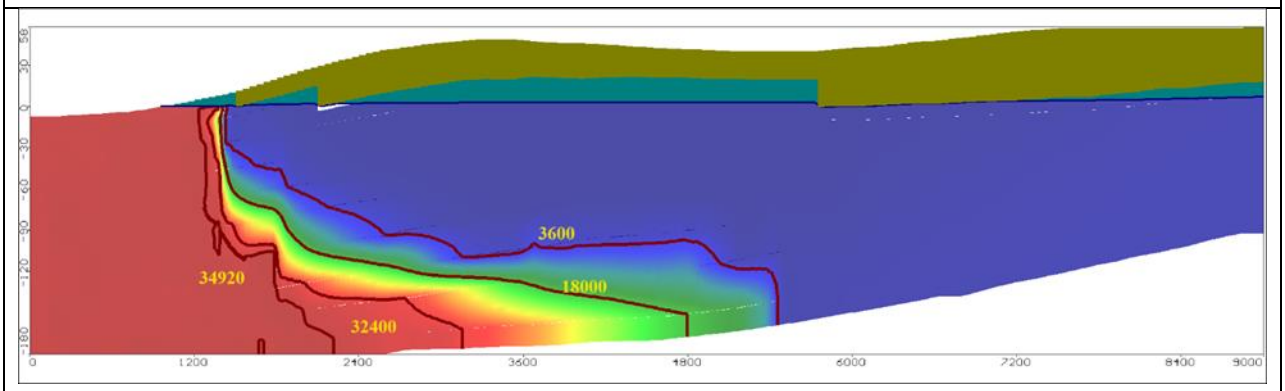

(b) SLR=0.5 m (X_t= 2216 m of 97% =34920 mg/L)

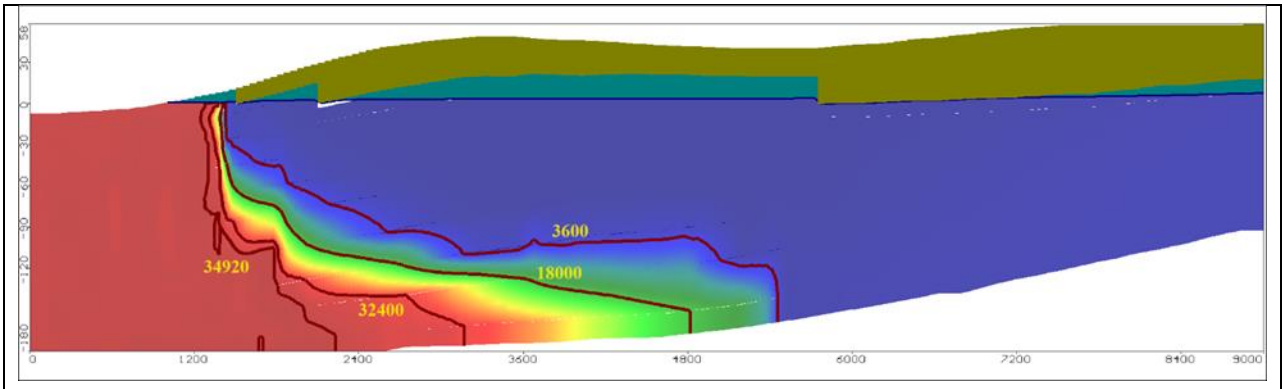

(c) SLR=1.0m (X_t= 2229 m of 97% =34920 mg/L)

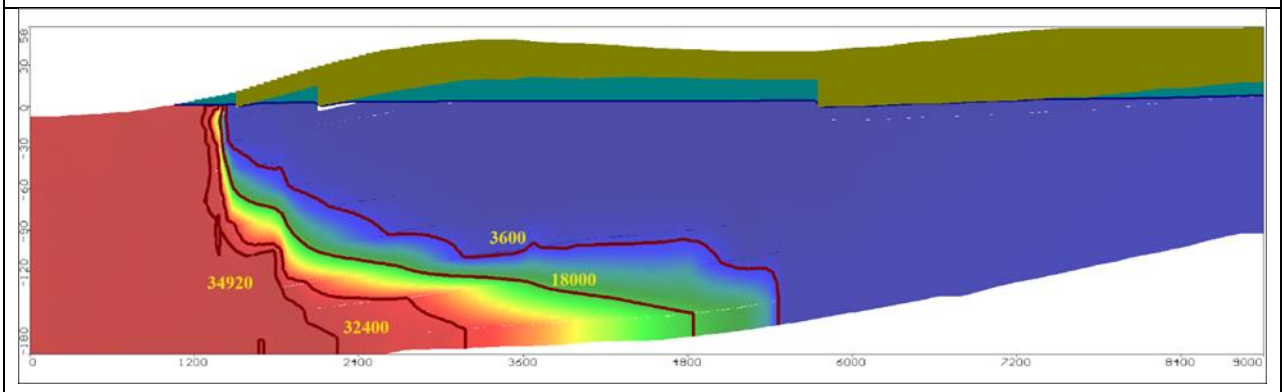

(d) SLR=1.5m (X_t= 2243 m of 97% =34920 mg/L)

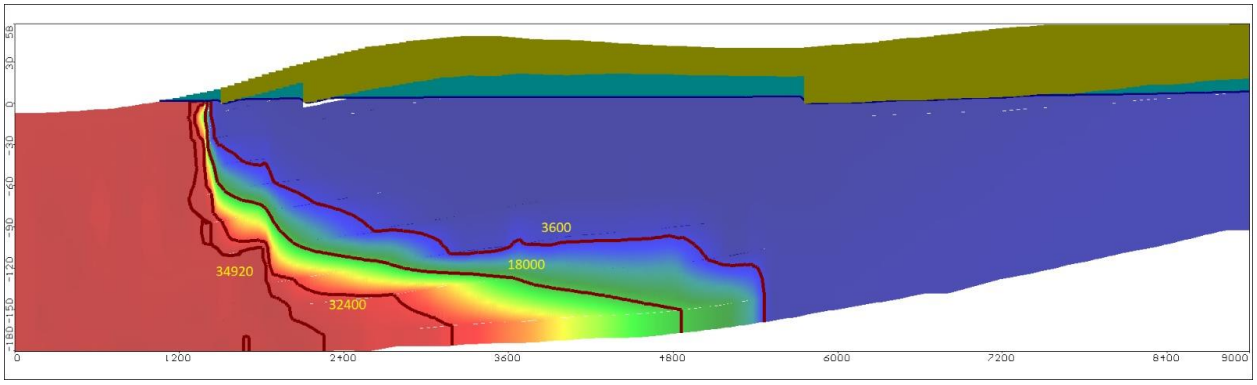

(e) SLR=2.0m (X_t= 2252 m of 97% =34920 mg/L)

Figure 8 Seawater intrusion distribution in Gaza coastal aquifer: (a) steady state condition, (b) SLR=0.5m, (c) SLR=1.0m, (d) SLR=1.5m, and (e) SLR=2.0m

5 Conclusion

This research displayed the variations of the seawater-freshwater interface using different available analytical solutions developed by Ghyben (1888), Glover (1959), Rumer Jr and Harleman (1963), and Verruijt (1968)

through web-based interface tool. The simulated intrusion length of seawater intrusion wedge by SEAWAT was compared with the analytical solutions of Ataie-Ashtiani et al. (2013) for constant flux boundary and constant head boundary problems. The seawater freshwater interface results were presented for two case studies including hypothetical unconfined coastal aquifer (Sun et al. 2021), and Gaza coastal aquifer through the built seawater-freshwater interface tool using JavaScript language. The calculated length of seawater wedge toe equals 375.021 m, 350.335 m, 350.09 m, and 382.75m for Gyhben Herzberg, Glover, Rumer-Herleman, and Virruijt respectively. The simulated value of toe length by Sun et al. 2021 for the same hypothetical unconfined coastal aquifer equals 340m. Comparing the results of available analytical solutions proved that Glover's solution (1959) and Rumer Jr and Harleman's (1963) solution are the most agreement with numerical one. The comparison between the intrusion length for the Gaza coastal aquifer by Ataie-Ashtiani et al. (2013) and the calculated estimated value through the web-based interface tool revealed a good agreement for sea level rise equals 2.0m and varied values of sea slope boundary. This conclusion holds true for the two case studies—constant head boundary and constant flow boundary—that are given. Increasing sea level rise led to the advance of the toe of the seawater intrusion wedge in the Gaza coastal aquifer. For various sea level rise scenarios in the Gaza coastal aquifer, the comparison of the simulated and calculated wedge toe penetration length revealed good agreement. For the designated SLR scenarios in the Gaza coastal aquifer, the estimated values of seawater intrusion toe length using the web-based tool equal 2101, 2119, 2137, 2155, and 2173 m, respectively. Conversely, for the designated SLR scenarios, the simulated values using the SEAWAT code equals 2216, 2229, 2243, and 2252 m, which is equivalent to 0.5, 1.0, 1.5, and 2.0, respectively. Overall, this study provides valuable insights into the intrusion of seawater into coastal aquifers. The findings of this research can be used to update regulations and management techniques to address and lessen the adverse impacts of this intrusion. Furthermore, using a web-based interface, the research investigates how Sea Level Rise (SLR) modifies the toe location of seawater intrusion in coastal aquifers.

Web-Based Seawater-Freshwater Interface Designed Model Link:

https://mselmy.github.io/Seawater-Freshwater-Interface-Web-Based-Model/index.html

Funding:

Financial support received from the STDF-Egypt (Grant number#46278) has facilitated this collaborative research as a part of a project titled “Optimal Exploitation Strategies for Sustainable Utilization of Fossil Groundwater Reserves in Egypt”.

ACKNOWLEDGMENTS

This paper is part of a project titled “Optimal Exploitation Strategies for Sustainable Utilization of Fossil Groundwater Reserves in Egypt” funded by the Science and Technology Development Fund (STDF), Egypt under a grant number (ID#46278).

REFERENCES

Abd-Elaty, I., Zelenakova, M., 2022. Saltwater intrusion management in shallow and deep coastal aquifers for high aridity regions. J. Hydrol. Reg. Stud. 40, 101026. https://doi.org/10.1016/j.ejrh.2022.101026

Abdoulhalik, A., Ahmed, A.A., 2017. The effectiveness of cutoff walls to control saltwater intrusion in multi-layered coastal aquifers: Experimental and numerical study. J. Environ. Manage. 199, 62–73. https://doi.org/10.1016/j.jenvman.2017.05.040

Abualtayef, M., Rahman, G.A., Snounu, I., Qahman, K., Sirhan, H., Seif, A.K., 2017. Evaluation of the effect of water management interventions on water level of Gaza coastal aquifer. Arab. J. Geosci. 10, 1–19. https://doi.org/10.1007/s12517-017-3329-x

Anderson, E.I., 2021. Analytical Solutions for Confined and Unconfined Coastal Interface Flow by the Hodograph Method. Water Resour. Res. 57. https://doi.org/10.1029/2021WR030323

Armanuos, A.M., Al-Ansari, N., Yaseen, Z.M., 2020a. Assessing the Effectiveness of Using Recharge Wells for Controlling the Saltwater Intrusion in Unconfined Coastal Aquifers with Sloping Beds: Numerical Study. Sustainability 12, 2685. https://doi.org/10.3390/su12072685

Armanuos, A.M., Al-Ansari, N., Yaseen, Z.M., 2020b. Underground Barrier Wall Evaluation for Controlling Saltwater Intrusion in Sloping Unconfined Coastal Aquifers. Water 12, 2403. https://doi.org/10.3390/w12092403

Armanuos, A.M., Ibrahim, M.G., Mahmod, W.E., Takemura, J., Yoshimura, C., 2019. Analysing the Combined Effect of Barrier Wall and Freshwater Injection Countermeasures on Controlling Saltwater Intrusion in Unconfined Coastal Aquifer Systems. Water Resour. Manag. 33, 1265–1280. https://doi.org/10.1007/s11269-019-2184-9

Ataie-Ashtiani, B., Werner, A.D., Simmons, C.T., Morgan, L.K., Lu, C., 2013. How important is the impact of land-surface inundation on seawater intrusion caused by sea-level rise? Hydrogeol. J. 21, 1673.

Chang, S.W., Clement, T.P., Simpson, M.J., Lee, K.-K., 2011. Does sea-level rise have an impact on saltwater intrusion? Adv. Water Resour. 34, 1283–1291. https://doi.org/10.1016/j.advwatres.2011.06.006

Dang, N.M., Vien, L.N., Tung, N.B., Duong, T.A., Dang, T.D., 2020. Assessments of Climate Change and Sea Level Rise Impacts on Flows and Saltwater Intrusion in the Vu Gia - Thu Bon River Basin, Vietnam, in: Trung Viet, N., Xiping, D., Thanh Tung, T. (Eds.), APAC 2019. Springer Singapore, Singapore, pp. 1367–1374. https://doi.org/10.1007/978-981-15-0291-0_185

Emara, S.R., Armanuos, A.M., Gado, T.A., Zeidan, B.A., 2023a. Verification of experimental saltwater intrusion interface in unconfined coastal aquifers using numerical and analytical solutions. Acque Sotter. - Ital. J. Groundw. 12, 23–38. https://doi.org/10.7343/as-2023-668

Emara, S.R., Armanuos, A.M., Shalby, A., 2024a. Appraisal seawater intrusion vulnerability for the Moghra coastal aquifer, Egypt– application of the GALDIT index, sensitivity analysis, and hydro-chemical indicators. Groundw. Sustain. Dev. 25, 101166. https://doi.org/10.1016/j.gsd.2024.101166

Emara, S.R., Armanuos, A.M., Zeidan, B.A., Gado, T.A., 2024b. Numerical investigation of mixed physical barriers for saltwater removal in coastal heterogeneous aquifers. Environ. Sci. Pollut. Res. 31, 4826–4847. https://doi.org/10.1007/s11356-023-31454-z

Emara, S.R., Gado, T.A., Zeidan, B.A., Armanuos, A.M., 2023b. Evaluating the Impact of Inclined Cutoff-Wall to Control Seawater Intrusion in Heterogeneous Coastal Aquifers. Water Resour. Manag. 37, 6021–6050. https://doi.org/10.1007/s11269-023-03641-7

Fan, Y., Lu, W., Miao, T., Li, J., Lin, J., 2020. Multiobjective optimization of the groundwater exploitation layout in coastal areas based on multiple surrogate models. Environ. Sci. Pollut. Res. 27, 19561–19576. https://doi.org/10.1007/s11356-020-08367-2

Ghyben, B.W., 1888. Nota in verband met de voorgenomen putboring nabij, Amsterdam. The Hague 21.

Glover, R.E., 1959. The pattern of fresh-water flow in a coastal aquifer. J. Geophys. Res. 64, 457–459.

Goswami, R.R., Clement, T.P., 2007. Laboratory-scale investigation of saltwater intrusion dynamics. Water Resour. Res. 43. https://doi.org/10.1029/2006WR005151

Guo, W., Langevin, C.D., 2002. User's guide to SEAWAT; a computer program for simulation of three-dimensional variable-density ground-water flow. https://doi.org/10.3133/twri06A7.

Heen, Z.H.A., Muhsen, S., 2016. Application of vertical electrical sounding for delineation of sea water intrusion into the freshwater aquifer of southern governorates of Gaza Strip, Palestine. IUG J. Nat. Stud. 24.

Herzberg, A., 1901. Die wasserversorgung einiger Nordseebader. J Gasbeleucht Wasserversorg 44, 842–844.

Javadi, A., Hussain, M., Sherif, M., Farmani, R., 2015. Multi-objective Optimization of Different Management Scenarios to Control Seawater Intrusion in Coastal Aquifers. Water Resour. Manag. 29, 1843–1857. https://doi.org/10.1007/s11269-015-0914-1

Kaleris, V.K., Ziogas, A.I., 2013. The effect of cutoff walls on saltwater intrusion and groundwater extraction in coastal aquifers. J. Hydrol. 476, 370–383. https://doi.org/10.1016/j.jhydrol.2012.11.007

Koussis, A.D., Mazi, K., Destouni, G., 2012. Analytical single-potential, sharp-interface solutions for regional seawater intrusion in sloping unconfined coastal aquifers, with pumping and recharge. J. Hydrol. 416–417, 1–11. https://doi.org/10.1016/j.jhydrol.2011.11.012

Kuan, W.K., Jin, G., Xin, P., Robinson, C., Gibbes, B., Li, L., 2012. Tidal influence on seawater intrusion in unconfined coastal aquifers. Water Resour. Res. 48. https://doi.org/10.1029/2011WR010678

Lu, C., Xin, P., Kong, J., Li, L., Luo, J., 2016. Analytical solutions of seawater intrusion in sloping confined and unconfined coastal aquifers. Water Resour. Res. 52, 6989–7004. https://doi.org/10.1002/2016WR019101

Lu, C., Xin, P., Li, L., Luo, J., 2015. Seawater intrusion in response to sea-level rise in a coastal aquifer with a general-head inland boundary. J. Hydrol. 522, 135–140.

Luo, Z., Kong, J., Shen, C., Lu, C., Xin, P., Werner, A.D., Li, L., Barry, D.A., 2022. Approximate analytical solutions for assessing the effects of unsaturated flow on seawater extent in thin unconfined coastal aquifers. Adv. Water Resour. 160, 104104. https://doi.org/10.1016/j.advwatres.2021.104104

Mehdizadeh, S.S., Badaruddin, S., Khatibi, S., 2019. Abstraction, desalination and recharge method to control seawater intrusion into unconfined coastal aquifers. Glob. J. Environ. Sci. Manag. 5. https://doi.org/10.22034/gjesm.2019.01.09

Motallebian, M., Ahmadi, H., Raoof, A., Cartwright, N., 2019. An alternative approach to control saltwater intrusion in coastal aquifers using a freshwater surface recharge canal. J. Contam. Hydrol. 222, 56–64. https://doi.org/10.1016/j.jconhyd.2019.02.007

Qahman, K., 2004. Aspects of Hydrogeology, Modeling, and Management of Seawater Intrusion for Gaza Aquifer–Palestine. Unpubl. Diss. PhD LIMEN Ecole Mohammadia 'Ingenieurs Univ. Mohammed V-Moroc.

Ranjbar, A., Mahjouri, N., Cherubini, C., 2020. Development of an efficient conjunctive meta-model-based decision-making framework for saltwater intrusion management in coastal aquifers. J. Hydro-Environ. Res. 29, 45–58. https://doi.org/10.1016/j.jher.2019.11.005

Rumer Jr, R.R., Harleman, D.R., 1963. Intruded salt-water wedge in porous media. J. Hydraul. Div. 89, 193–220.

Sherif, M., Sefelnasr, A., Ebraheem, A.A., Javadi, A., 2014. Quantitative and Qualitative Assessment of Seawater Intrusion in Wadi Ham under Different Pumping Scenarios. J. Hydrol. Eng. 19, 855–866. https://doi.org/10.1061/(ASCE)HE.1943-5584.0000907

Sun, Q., Zheng, T., Zheng, X., Walther, M., 2021. Effects of subsurface barriers on seawater intrusion and nitrate accumulation in coastal aquifers. Authorea Prepr.

Verruijt, A., 1968. A note on the Ghyben-Herzberg formula. Hydrol. Sci. J. 13, 43–46.

Werner, A.D., Bakker, M., Post, V.E.A., Vandenbohede, A., Lu, C., Ataie-Ashtiani, B., Simmons, C.T., Barry, D.A., 2013. Seawater intrusion processes, investigation and management: Recent advances and future challenges. Adv. Water Resour., 35th Year Anniversary Issue 51, 3–26. https://doi.org/10.1016/j.advwatres.2012.03.004